ASTRONOMY & ASTROPHYSICS
SUPPLEMENT SERIES

Astron. Astrophys. Suppl. Ser. **128,** 349-357 (1998)

Searching for old neutron stars with ROSAT

II. Soft X-ray sources in galactic dark clouds

R. Danner[1,2]

[1] Max-Planck-Institut für Extraterrestrische Physik, Giessenbachstraße, 85748 Garching, Germany
[2] Palomar Observatory, California Institute of Technology, Pasadena, CA 91125, USA

Received December 16, 1996; accepted August 1, 1997

Abstract. This is the second in a series of three papers constraining the number of detectable old neutron stars in the Galaxy. Here, I present the statistical analysis of a sample of X-ray sources coincident with areas of dark clouds in the Galactic plane. I compare this sample with all sources in the ROSAT All-Sky Survey bright source catalog within 20° of the Galactic plane. I present the results of an identification program of a subset of sources that are compatible with a soft, thermal X-ray spectrum and an effective source temperature of less than 70 eV. The three brightest sources in this sample form an intriguing subgroup. One of them is a previously identified candidate for an accreting neutron star. I identify the other two sources with hot white dwarf stars. I find no new accreting neutron star candidate in this sample. Based on this result, I derive an upper limit to the space density of accreting neutron stars in fields of Galactic dark clouds of $\sim 2\,\mathrm{sr}^{-1}$ at a count rate $> 0.05\,\mathrm{s}^{-1}$.

Key words: surveys — X-rays: stars — stars: neutron; white dwarfs

1. Old neutron stars in the galactic plane

The discovery of surface emission from old isolated neutron stars has long been regarded as a key to the understanding of their equation of state and has caused a wealth of theoretical work over the last three decades, see e.g. (Ostriker et al. 1970; Helfand et al. 1980). Old isolated neutron stars were predicted to be visible as soft X-ray sources within the reach of current satellite missions, see Treves & Colpi (1991), Blaes & Madau (1993) and also (Madau & Blaes 1994; Colpi et al. 1993). Recently, three sources have been suggested to be actual detections of old neutron stars accreting from the interstellar medium (Stocke et al. 1995; Walter et al. 1996; Haberl et al. 1996). However, the number of candidates for accreting neutron stars fall surprisingly short of the most conservative estimates. Paper I (Danner 1998) described a comprehensive identification program of sources in molecular clouds at high galactic latitude aimed at the systematic search for such objects. Please see Paper I for a brief introduction to accreting neutron stars.

In the present paper, I describe a survey of a large area in the galactic plane coincident with galactic dark clouds. These areas are most promising for the detection of old neutron stars accreting from the interstellar medium because: (1) only the slow members of the total neutron star population are expected to accrete and will be therefore concentrated toward the Galactic plane; (2) the clouds with their high densities of gas and dust provide ample material for accretion; (3) these clouds occupy a much larger volume than the local molecular clouds we find at high Galactic latitudes; and (4) the high extinction through dark clouds obscures background sources and reduces so the number of chance coincidences.

These favorable conditions entail three limitations: (1) the stellar density in the Galactic plane is very high. In most situations several objects are found within a typical error circle of 30 arcsecond. As a consequence, optical spectroscopy is required to resolve ambiguities already on a bright optical level. Very deep searches ($m_V > 20$) are feasible only with significantly smaller error circles. (2) Dark clouds fill a large fraction of the entire Galactic plane and are not easily surveyed by any telescope. A systematic search will quickly grow into a project too large to manage within a realistic time frame. (3) The softest sources, deep inside a cloud will suffer substantial absorption from the material in the immediate vicinity of the source.

Two groups have recently published studies of ROSAT sources in a subset of galactic dark clouds. See Motch et al. for a comprehensive list of identifications in Cygus (1997a,b) and Belloni et al. (1997) for an identification of further candidate objects in the Cygnus and Cygnus OB7 region.

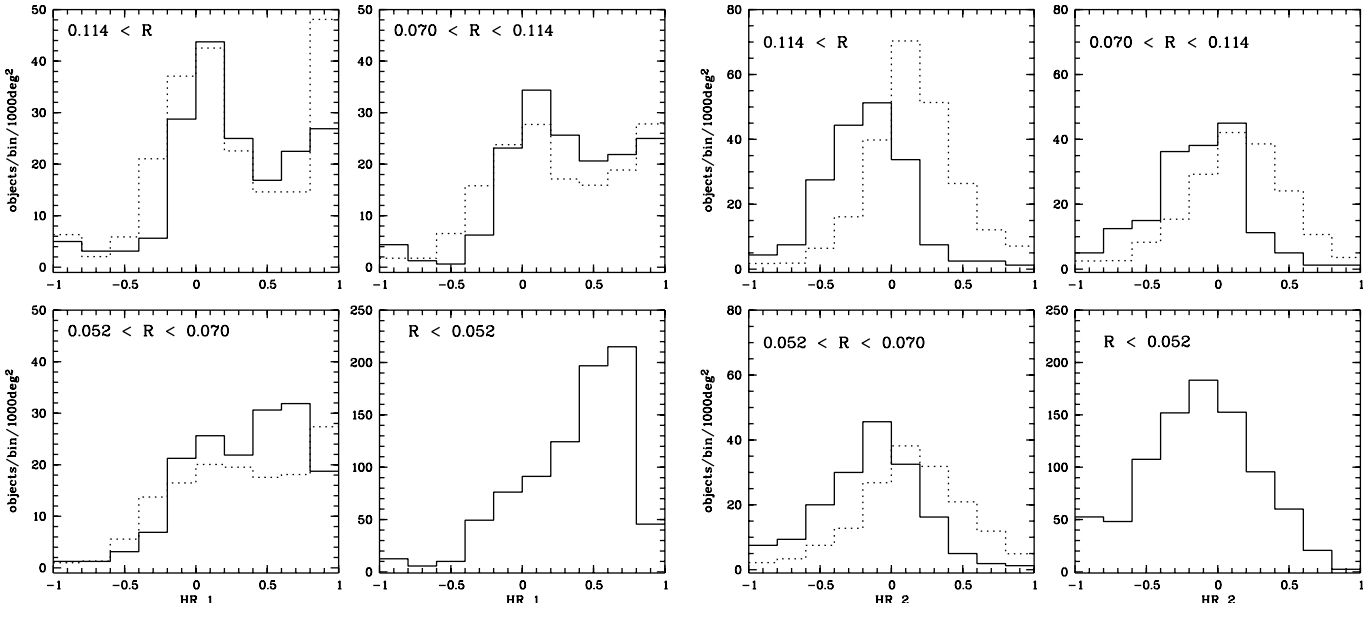

Fig. 1. The evolution of HR1 (left) and HR2 (right) with the source count rate in the dark cloud sample (solid line) as compared to the total galactic sample (dotted line). The histograms show the number of sources per 1000 deg^2 per hardness ratio interval. R gives the count rate in counts per second

I have analyzed the statistical properties of a sample of bright X-ray sources coincident with the clouds identified by Dame et al. (1987) and compared this sample with the average population in the galactic plane. From the dark cloud sample I selected a small group of sources that stand out on their X-ray properties. I studied these sources in detail through optical imaging and spectroscopy. The three brightest sources in this sample have exciting properties. One of them is an independently rediscovered neutron star candidate. The other two sources are identified with hot white dwarf stars.

2. The dark cloud sample

Dame et al. (1987) have collected a comprehensive list of dark clouds in the Galaxy. Their survey was based on the detection of emission at 115 GHz, the frequency of the $0 \rightarrow 1$ rotational transition of CO. This spectral line is a standard tracer of dense molecular gas. I used the coordinates provided by Dame et al. (1987). Table 1 lists all these clouds with the boundaries in Galactic coordinates.

Five cloud complexes have been excluded from the original list. The Lindblad Ring and the "−12 km/s" clouds are irregular and poorly defined. The Aquila Rift, Per OB2 and ρ Oph were also excluded because they extend over a large area on the sky and appear to consist of smaller cloudlets. The area included in the survey covers approximately 1600 deg^2. The standard analysis of the ROSAT All-Sky survey finds 2270 source within this area above a maximum likelihood threshold of 10. This source list is based of the first processing of the survey at MPE (Voges 1993). All sources found inside the areas of Table 1 were included in the list of dark cloud sources.

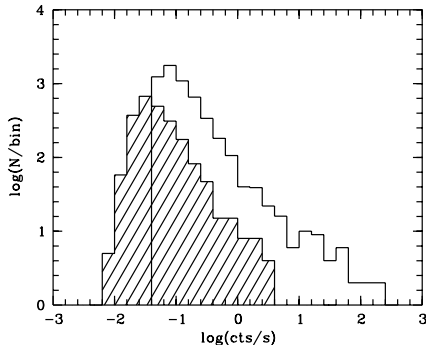

Fig. 2. Logarithmic distribution of the number of detected sources versus the count rate for sources in the galactic plane (open histogram) and the dark cloud sample (hashed histogram). The galactic sample shows an artificial cut-off at $0.05\,\mathrm{s}^{-1}$. The slope of the galactic sample is −0.57, slightly steeper than −0.5 as expected for a uniform distribution in Euclidean space

3. Statistical analysis of the source sample

The standard processing of the ROSAT All-Sky Survey gives in addition to the position of the source the detected count rate and two hardness ratios as an estimator of the spectrum of the source.

Table 1. Areas in the Galactic plane that define the dark cloud sample (Dame et al. 1987): name of cloud, boundaries in Galactic longitude (l) and latitude (b), approximate size. The often complex shape of the clouds was approximated with a rectangle, thereby including an area larger than the actual cloud.

Name	$l_{\min}$	$l_{\max}$	$b_{\min}$	b_{max}	Size
Cloud A	44.0	49.5	−4.0	2.0	$5.5° \times 6°$
Cloud B	44.0	54.0	−4.0	5.0	$1° \times 9°$
Cloud C	50.0	55.0	−1.0	3.5	$5° \times 4.5°$
Vul Rift	54.0	63.0	−3.0	5.0	$9° \times 8°$
Cyg Rift	63.0	86.5	−4.0	4.0	$23.5° \times 8°$
Cyg OB7	87.0	99.0	−3.0	8.0	$12° \times 11°$
Cepheus	100.0	120.0	11.0	22.0	$19° \times 11°$
Taurus	163.0	178.0	−22.0	−9.5	$14° \times 12.5°$
Mon OB1	197.5	205.0	−1.0	4.0	$7.5° \times 5°$
Orion A	208.5	218.0	−21.0	−14.5	$9° \times 6.5°$
Orion B	202.5	208.0	−21.0	−6.0	$5.3° \times 15°$
Mon R2	210.0	218.0	−14.0	−10.0	$7.8° \times 4°$
Vela Sheet	272.0	279.0	−3.0	8.0	$7° \times 11°$
Cham	295.0	305.0	−20.0	−12.0	$9.6° \times 8°$
Coalsack	300.0	307.0	−4.0	3.0	$7° \times 7°$
G317-4	315.0	320.0	−6.0	−2.0	$5° \times 4°$
Lupus	333.0	346.0	4.0	22.0	$12.7° \times 18°$
R Cr A	357.0	4.0	−22.0	−14.0	$6.7° \times 8°$

The ROSAT pass band from 0.1 to 2.0 keV can be split into four bands according to their Pulse Height Amplitude channels (PHA). Three of these bands are independent: $A(0.1-0.4\,\mathrm{keV}$; PHA $11-40)$, $B(0.5-2.0\,\mathrm{keV}$; PHA $50-200)$, $C(0.5-0.9\,\mathrm{keV}$; PHA $50-200)$ and $D(0.9-2.0\,\mathrm{keV}$; PHA $90-200)$. The two ROSAT hardness ratios HR1 and HR2 are defined as the ratios of the number of detected photons in the respective band:

$$\mathrm{HR1} = \frac{B-A}{B+A}; \qquad \mathrm{HR2} = \frac{D-C}{D+C}.$$

A soft source, dominated by photons in the soft band, has a negative hardness ratio, whereas a hard source has a positive value in its hardness ratio.

I was interested in how the distribution of the two hardness ratios HR1 and HR2 evolves with count rate. I split my dark cloud sample into four count rate intervals so that the number of sources per interval was approximately equal. I then computed hardness ratio histograms with a bin width of 0.2. I finally normalized the histograms to the number of sources per $1000\,\mathrm{deg}^2$. The histograms for the two hardness ratios are shown in Fig. 1.

Part of the obvious increase of harder sources with reduced count rate is instrumental. The combination of the ROSAT telescope and the proportional counter is most sensitive to photons around 1 keV. Additionally, the point-spread function at higher energies is more narrow. This leads to a higher detection probability for harder sources in the source detection algorithm. A reliable estimate of these instrumental effects is difficult to access without extensive modeling of the detector and the source detection algorithm. I have therefore resolved to comparing the dark source sample with the average population of ROSAT sources in the galactic plane. Because these two samples differ only in their location on the sky, they will be equally affected by the instrumental response.

I used the ROSAT bright source catalog to select a galactic reference sample. The ROSAT bright source catalog was published by Voges et al. (1996) based on the ROSAT All-Sky Survey. A total of 18,811 sources were detected above a limiting count rate of $0.05\,\mathrm{s}^{-1}$. Of these 8547 sources are brighter than $0.1\,\mathrm{s}^{-1}$. At this count rate level, the survey has a sky coverage of 92 percent (Voges et al. 1996). From this bright source list I selected all sources within 20° of the Galactic plane. Of 18,811 sources in the bright source list, 5540 sources lie within $|b| < 20°$.

I binned this much larger source sample in the same way as the dark cloud sample. The histograms of the galactic sample are plotted in Fig. 1 with a dotted line. Due to the cut off at a rate of $0.05\,\mathrm{s}^{-1}$ the galactic sample is only shown in the three brighter count rate intervals. Sources with count rates $> 0.05\,\mathrm{s}^{-1}$, that lie inside the dark cloud fields, are in both source samples.

Figure 2 shows the total distribution of count rates in the two samples. The dark cloud sample extends to lower count rates than the galactic sample from the bright source list. Due to the larger sampling area for the galactic sample there are a larger number of sources and more objects at the bright end of the distribution. The slopes of the two distributions are within the uncertainties the same. Both distributions are slightly steeper, −0.57 compared to −0.5, than expected for a uniform distribution in Euclidean space. This indicates that there is an excess of faint sources over the extrapolation from local sources.

The dark cloud sample contains 894 sources above a count rate of $0.05\,\mathrm{s}^{-1}$ within $1600\,\mathrm{deg}^2$. The bright source list contains 5540 sources above the same count rate threshold within $9170\,\mathrm{deg}^2$ ($|b| < 20°$). Thus I obtain a source density of $0.56\,\mathrm{deg}^{-2}$ and $0.6\,\mathrm{deg}^{-2}$ respectively.

The two populations evolve quite similarly with count rate (see Fig. 1). However at all count rate levels there is an excess of the hardest sources in the galactic sample compared to the dark cloud sample. A possible interpretation of this behavior are hard background sources that are screened out in the dark cloud sample due to the high extinction through the could.

The evolution in HR2 is quite different for the dark cloud sample and galactic sample. In all three count rate intervals the dark cloud sample shows a significant shift to softer sources. This is the opposite result that one would expect from a single source population, distributed isotropically in in the sample volume, differing only in absorption. I suggest that there are two populations present in this sample. A group of hard, distant sources that lie beyond the galactic dark clouds as indicated by the evolution in HR1. A second group of softer sources, preferentially coinciding with galactic dark clouds, dominates the evolution in HR2. However, these softer sources are not

sufficiently soft to suggest the presence of accreting compact objects. More likely, they are due to coronal emission from stars.

4. Optical identification of soft sources

From the list of sources that are found in the fields of Table 1, I selected all sources that are compatible with a soft, thermal source spectrum. Paper I showed that HR2 is a better estimator for the softness of a source spectrum because it suffers less from intervening absorption. Sources with a black body spectrum and a source temperature of 70 eV or less will have a hardness ratio HR2 of -0.8 or less, if they penetrate less than $N_{\rm H} = 10^{21}\,{\rm cm}^{-2}$. Neutron stars accreting from the interstellar medium are not expected to show harder source spectra (e.g. Blaes & Madau 1993). Some authors, e.g. Zamperi et al. (1995), have argued that the emergent spectrum of accreting neutron stars might have a hard component but the bulk of the emission ($> 80\%$) is still equivalent to a soft thermal spectrum.

4.1. Selection criteria

A conservative selection criterion for soft sources would require that the hardness ratio plus its error is less than some threshold, $\mathrm{HR2} + \Delta\mathrm{HR2} \leq \mathrm{HR2}_{\rm max}$. However, this criterion is too stringent for my sample. Soft sources that are only detected in the soft band and are not detected in the hard band are assigned by the standard processing an artificially large error in the hardness ratio. Applying the above selection criterion would exclude all these sources. Instead, I define a filter based on source brightness. I have selected all sources with a rate $> 0.05\,{\rm s}^{-1}$ and at least 20 detected counts. A minimum of 20 counts gives a reasonable confidence in the accuracy of the hardness ratio, and the count rate limit guarantees an area coverage of better than 92%.

Out of 2270 source in my dark cloud sample only 16 sources pass this selection filter. Table 2 lists all 16 sources with their ROSAT name, coordinates and their X-ray parameters. I have approximated the boundaries of the dark clouds with a wide rectangle. Therefore some of the sources in this areas might not be in front of a cloud and extragalactic objects might shine through gaps between individual cloudlets. A reduced stellar density close to the source position is a good indicator for the presence of a dark cloud.

4.2. The soft sub-sample

I have used the digitized sky-survey to create finding charts for each of the 16 sources, Fig. 3. A circle with a radius of $30''$ is centered in each figure at the X-ray position. Because most sources in the sample are faint, their uncertainty in the X-ray position is dominated by systematics. $30''$ is generally considered a conservative choice and supported by recent identification programs (see Paper I for more details). For some fields capital letters identify objects that have been further studied with optical spectroscopy.

All source positions were searched in the SIMBAD and NED catalogs for known counterparts. The result of this search is summarized in Table 2. Eight sources are identified with bright stars. For four additional fields, I conducted optical spectroscopy at the Palomar 60-inch and the Palomar 200-inch telescope. Low resolution spectra of candidates are shown in Fig. 4.

RX J0605.0 − 0707A is an AGN with a redshift of 0.233. RX J0620.2 − 0904A is a M dwarf star with H_α emission; the second object within the error circle RX J0620.2 − 0904B shows a stellar spectrum without emission lines. I therefore suggest the M dwarf to be the source of RX J0620.2 − 0904. RX J1922.7 + 0950 is identified as G star. No spectroscopic data is available for RX J2019.6 + 4048. However, Fig. 5 shows CCD frames in the Kron-Cousin B and R filter of this field. In the R image, a faint red object close to the X-ray position is apparent. An inspection of the R and B plate of the second generation of the Palomar Sky Survey (POSSII) yielded another red object coincident with RX J2114.6+4607, see mark on finding chart in Fig. 3. Pending identification through spectroscopy, I suggest that those two red objects are the likely extragalactic counterparts to RX J2019.6+4048 and RX J2114.6+4607.

Unfortunately there is no spectroscopic data available for RX J1958.6+7218. However, due to the moderately hard spectrum, the low count rate of $0.062\,{\rm s}^{-1}$ and the presence of object A inside the error circle I expect this source to be due to coronal emission from A.

4.3. The brightest sources

The three brightest sources in the sub-sample, RX J0550.6+0005, RX J1856.6−3754 and RX J1947.4+3045, are also the sources with the softest HR1 values. This indicates that they are affected very little by absorption. The brightest source RX J1856.6-3754 with $\approx 3.5\,{\rm s}^{-1}$ has been indeed suggested by Fred Walter et al. (1996) to be a nearby isolated neutron star, accreting from the interstellar medium. RX J0550.6+0005 is the known hot white dwarf star GD257 (Bergeron et al. 1994) with an effective surface temperature of $T_{\rm eff} = 45748\,{\rm K}$ also visible as EUV source (Marsh et al. 1997).

This left the intriguing case of RX J1947.4+3045 with very similar X-ray properties as GD257 but a much fainter optical counterpart ($m_V > 19$ compared to $m_V = 15.1$ for GD257). A comparison of the B and I plate of POSSII showed a very blue object within the X-ray error circle, see mark on finding chart in Fig. 3. I was able to obtain a spectrum of the source taken with the Palomar Hale telescope and the double spectrograph in June 1997, see Fig. 6. The spectrum is similar to that of a hot white dwarf star. It shows a hot continuum, no emission lines,

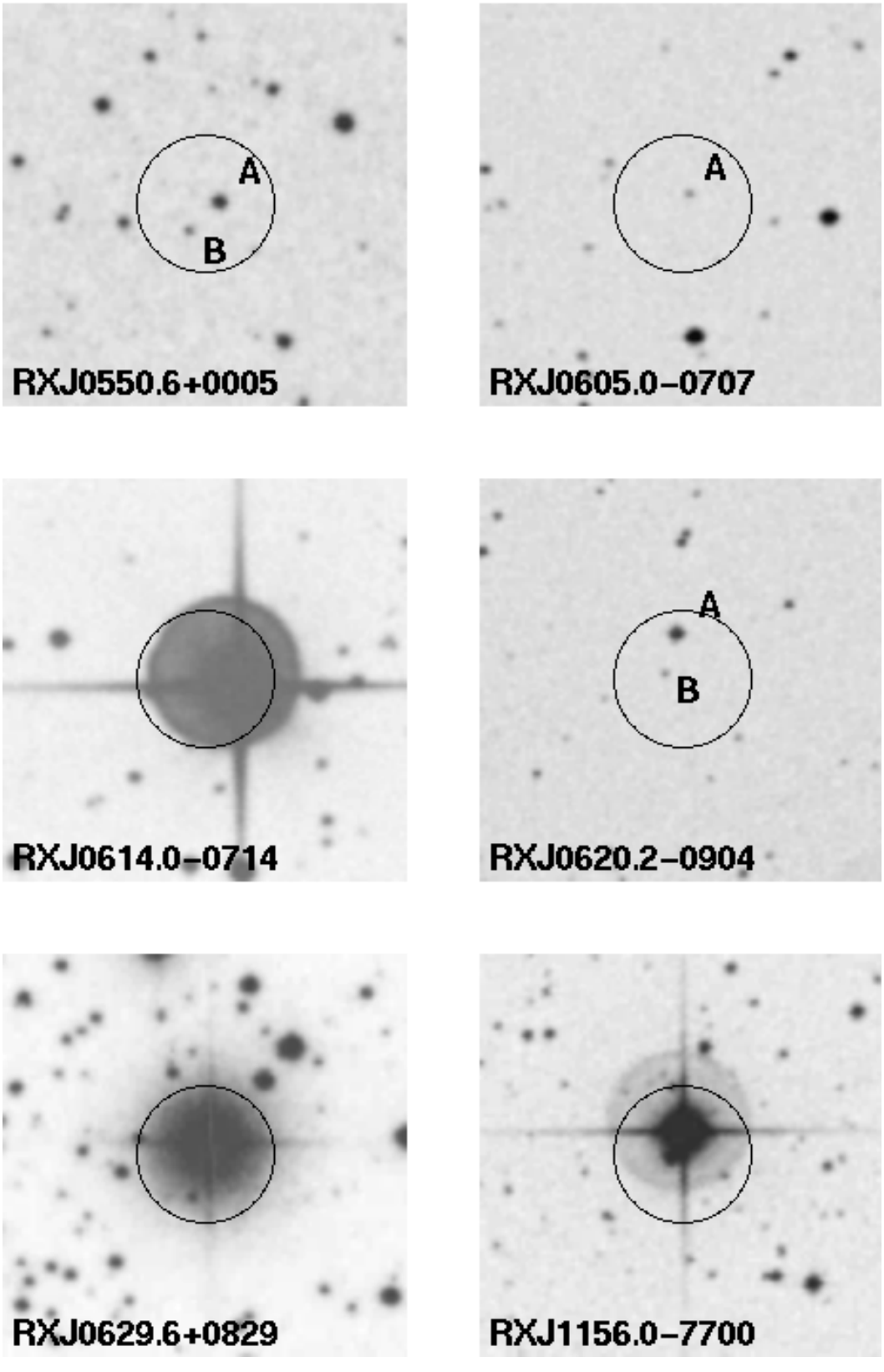

Fig. 3. Finding charts for soft sources. The charts have been produced from the digitized Palomar Sky-Survey. The circles are centered at the X-ray position and have a radius of 30 arcseconds. North is up and East to the left. Capital letters identify the brightest objects next to them

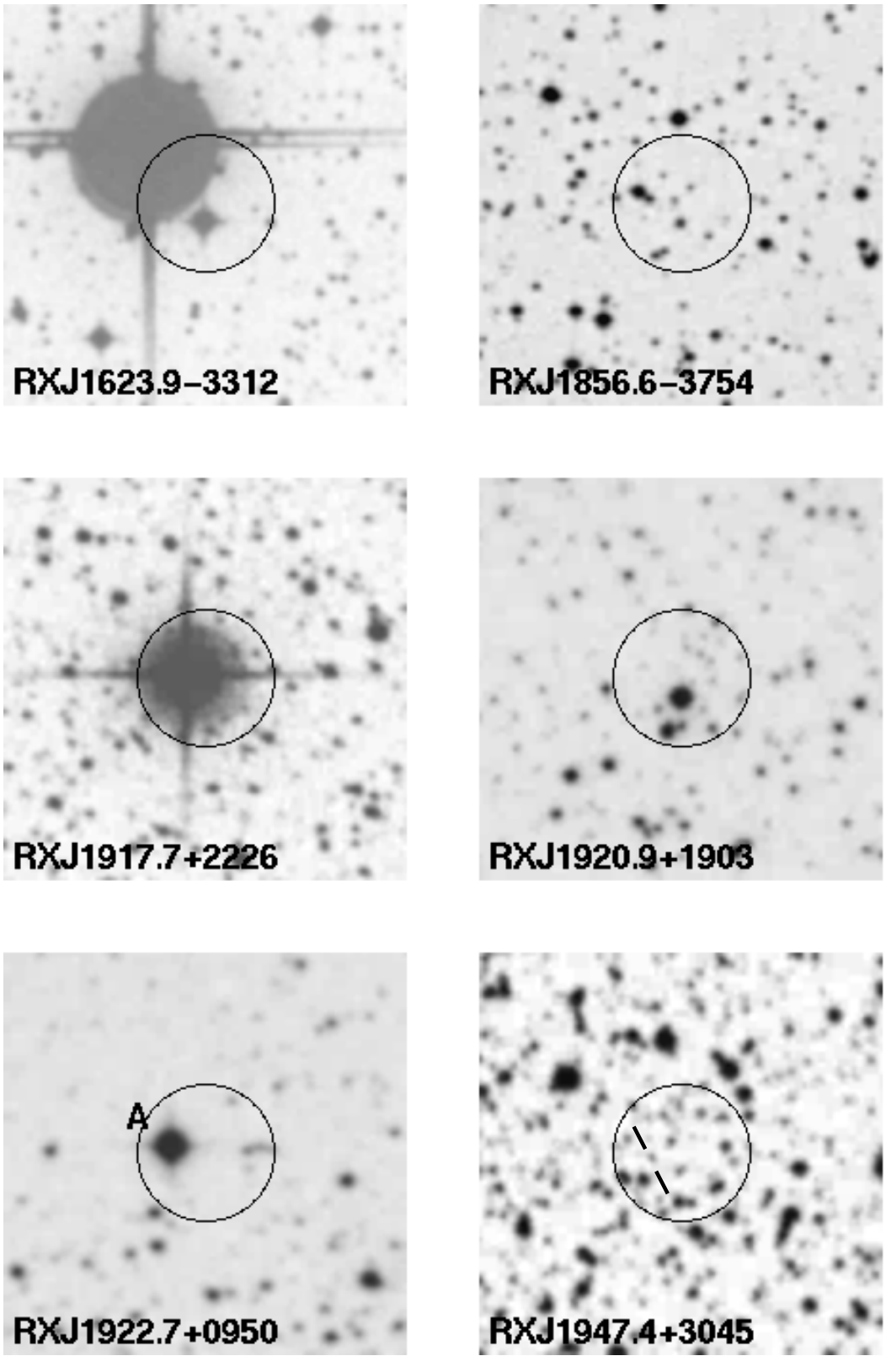

Fig. 3. continued

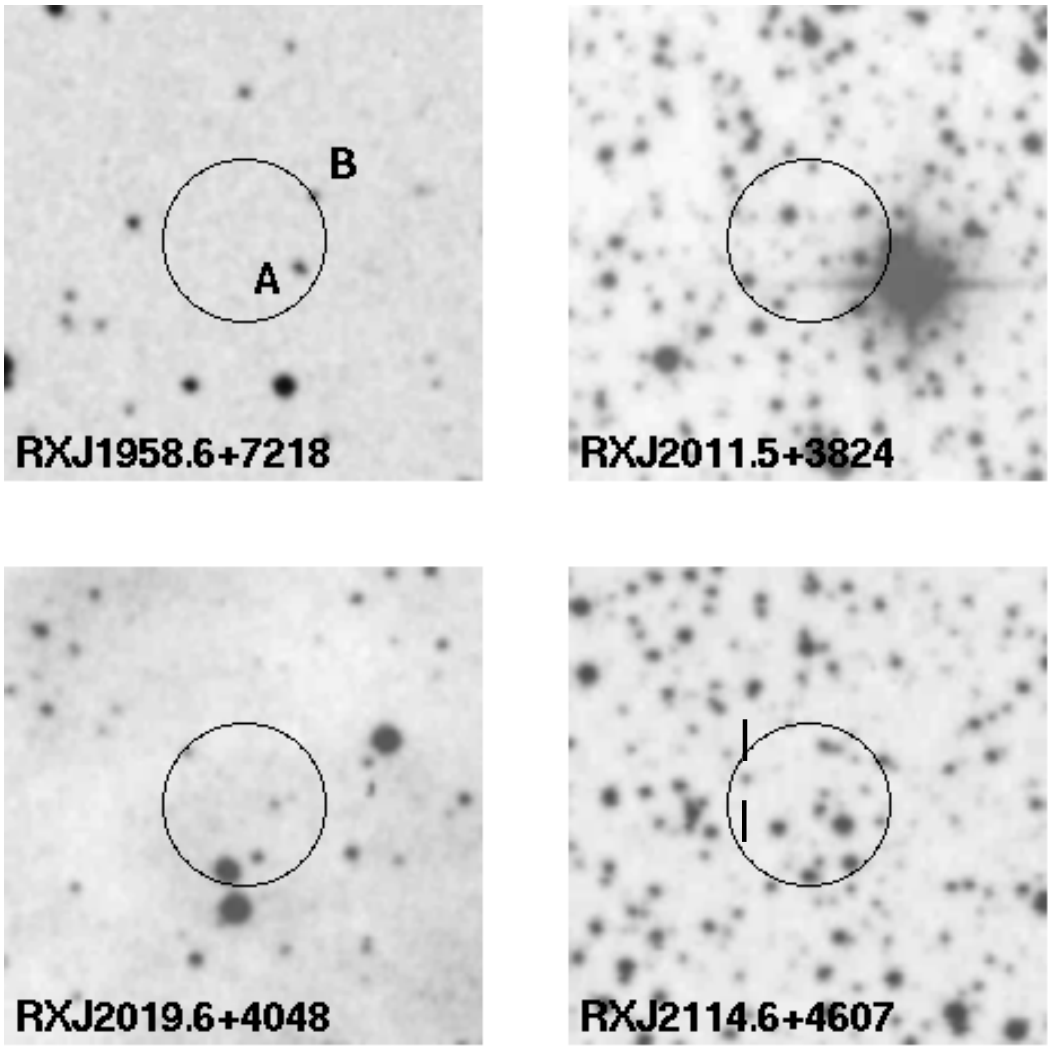

Fig. 3. continued

very weak Balmer lines in absorption and broad absorption bands that resemble Swan C_2 bands, due to molecular carbon. The hot continuum and the molecular bands give conflicting informations on the source temperature, demanding high and low surface temperatures simultaneously. This suggests that we are either looking at a binary system or absorption from circumstellar material. None of the models is particular conclusive. I am therefore not yet able to describe all features in the spectrum with a consistent model. This interesting object will be discussed in detail in a forthcoming letter.

5. Conclusion

I have reported on the statistical analysis of all sources in the ROSAT All-Sky Survey that are in areas identified by Dame et al. (1987) as Galactic dark clouds. Optical identifications for all sources with HR2 < -0.8 that meet a brightness limit, are presented. The majority coincide with bright, nearby stars. All but one source, have likely optical identifications. The source without plausible optical identification is also the brightest X-ray source. This source has been suggested earlier to be due to an nearby isolated neutron star accreting from the interstellar medium (Walter et al. 1996). The source stands out prominently among its peers and is easily rediscovered. I conclude that there is no similar source found in the sample. The dark cloud sample covered more than $1600\,\mathrm{deg}^2$ on the sky down to a limiting count rate of $0.05\,\mathrm{s}^{-1}$. One such source per $1600\,\mathrm{deg}^2$ corresponds to $6.25\ 10^{-4}\mathrm{deg}^{-2}$ or $\sim 2\,\mathrm{sr}^{-1}$ at a count rate $> 0.05\,\mathrm{s}^{-1}$. The detection limit in the All-Sky Survey is significantly lower than the cut-off chosen here. The statistical analysis shows no evidence of an increase of soft sources at lower count rates. I take this as further evidence that the derived limit is conservative and may be in fact much lower. An in depth analysis of this survey and Paper I will be published as Paper III.

Table 2. All soft sources in the dark cloud sample that match the brightness criterion (see text). Left to right columns: ROSAT name; X-ray source coordinates in epoch 2000.0; ROSAT count rate; total number of detected counts; hardness ratio 1 and 2; SIMBAD name of proposed optical counterpart (spec: optical spectrum presented in this paper); spectral type and optical magnitude of counterpart or remark

	X-ray Coordinates		Rate	Cnts	HR1	HR2	ID	Type	m_V
Name	$\alpha_{(2000)}$	$\delta_{(2000)}$	s^{-1}						
RX J0550.6+0005	05:50:37.7	+00:05:56	0.866	430	−0.98	−1.00	GD 257	DA1	15.10
RX J0605.0−0707	06:04:58.8	−07:07:06	0.038	20	0.79	−1.00	spec	AGN, $z = 0.233$	
RX J0614.0−0714	06:13:58.1	−07:14:50	0.092	24	0.06	−1.00	HD43066	B9	6.7
RX J0620.2−0904	06:20:11.5	−09:04:26	0.096	29	−0.01	−1.00	spec	dMe	
RX J0629.6+0829	06:29:37.0	+08:29:29	0.110	51	−0.25	−1.00	HD45759	F8	7.5
RX J1156.0−7700	11:55:57.7	−77:00:40	0.065	21	−0.67	−1.00	HD103673	G5V	8.6
RX J1623.9−3312	16:23:54.7	−33:12:28	0.060	23	−0.09	−0.82	HR6097	A0V+	7.0
RX J1856.6−3754	18:56:34.4	−37:54:26	3.456	567	−0.73	−0.92		NS candidate	
RX J1917.7+2226	19:17:39.3	+22:26:28	0.034	21	0.89	−1.00	HD180939	B5V+	6.9
RX J1920.9+1903	19:20:51.4	+19:03:44	0.070	40	−0.27	−1.00	1E1918.7+1857	dMe	
RX J1922.7+0950	19:22:40.7	+09:50:55	0.202	43	1.00	−1.00	spec	G star	
RX J1947.4+3045	19:47:23.3	+30:45:58	0.873	197	−0.95	−1.00	spec	hot white dwarf?	
RX J1958.6+7218	19:58:34.1	+72:18:24	0.062	52	−0.03	−0.85		probably stellar	
RX J2011.5+3824	20:11:28.3	+38:24:12	0.087	33	−0.02	−1.00	HD192020	G8V	7.93
RX J2019.6+4048	20:19:38.8	+40:48:25	0.230	63	0.85	−1.00		faint red object	
RX J2114.6+4607	21:14:33.6	+46:07:44	0.135	39	0.96	−0.86		faint red object	

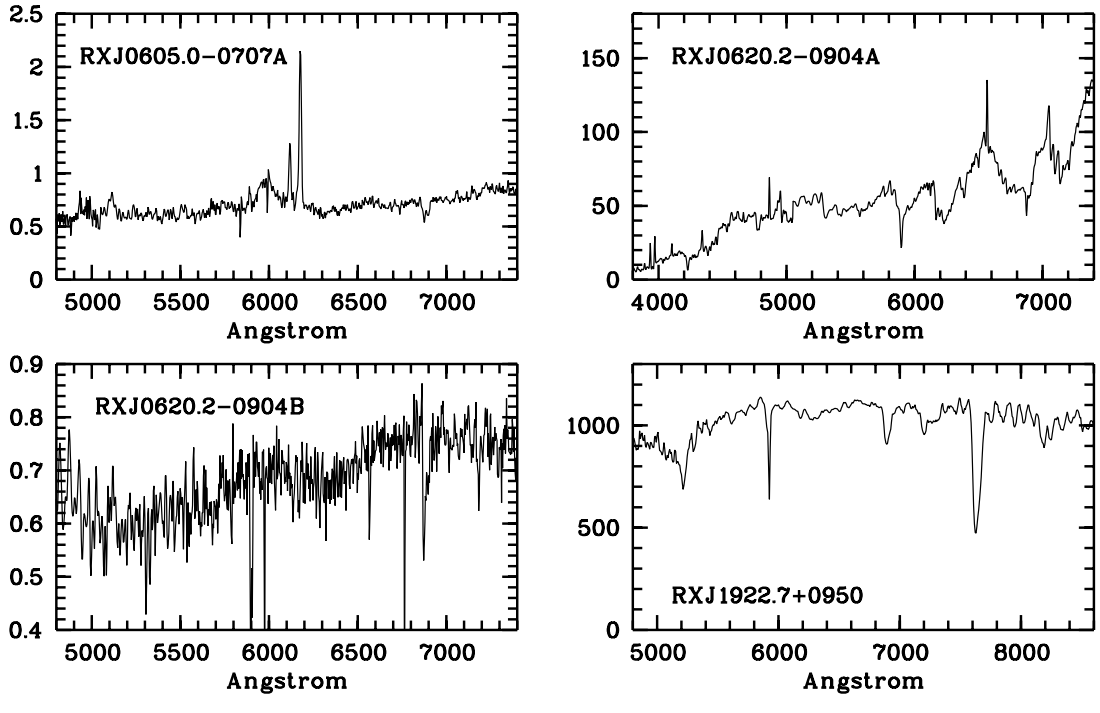

Fig. 4. Identification spectra for 4 objects. RX J0620.2 − 0904A: M dwarf with H_α emission. RX J0620.2 − 0904B: faint stellar object RX J0605.0 − 0707A: AGN with [OIII] and broad H_β emission at $z = 0.2$. RX J1922.7 + 0950: G star. The X-axes are in Angstrom and the Y-Axes in arbitrary units

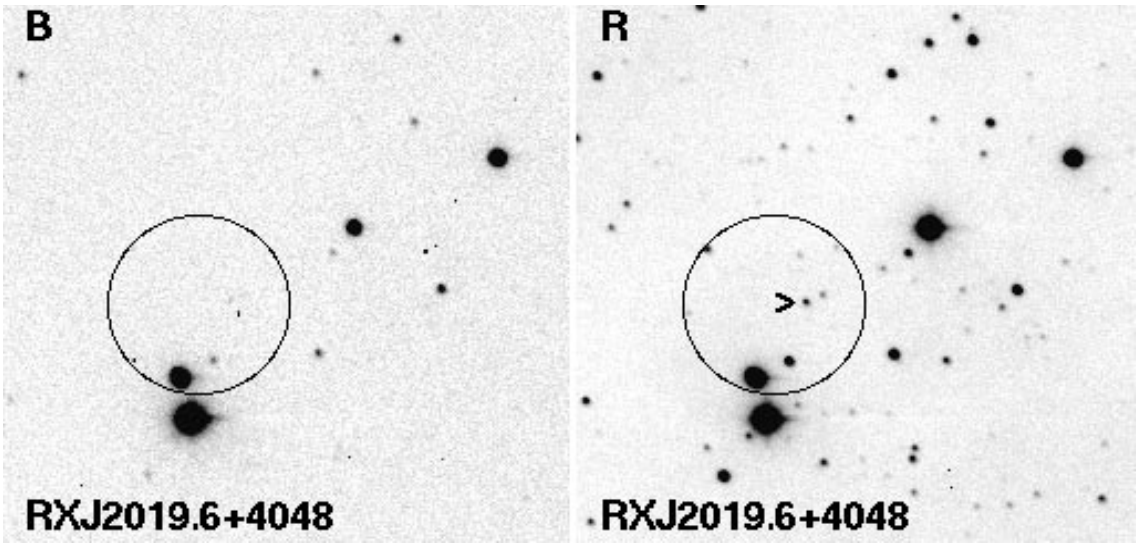

Fig. 5. CCD frames of the field of RX J2019.6+4048. The images were taken with 60 seconds integration time at the Palomar 60-inch telescope. The images are in the blue Kron-Cousin B (left) and R filter (right). An arrow in the read image marks a faint red object, probably an extragalactic object. The circles are centered at the X-ray source position and have a radius of 30 arcseconds. North is up and East to the left

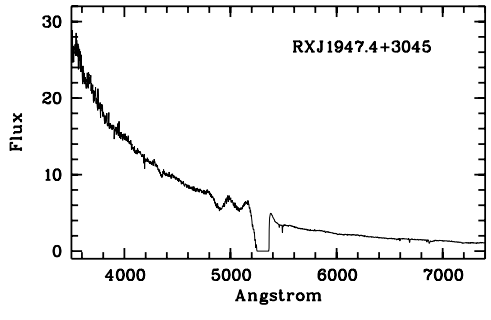

Fig. 6. Spectrum of the blue object inside the error box of RX J1947.4+3045. The gap in the spectrum around 5300 Å is caused by the lack of overlap between the red and the blue side of the spectrograph. The spectrum immediately next to the gap is heavily affected by effects of the dichroic that can not be calibrated. The Y-Axis has arbitrary units

Acknowledgements. This article is based on research conducted during my three year visit to the California Institute of Technology. I want to thank Prof. S.R. Kulkarni for his hospitality, support and countless discussions during this time. I am indebt to J. Trümper for his support of this project and many fruitful suggestions. I thank Chris Clemens and Angela Putney for help with understanding the blue spectrum. The ROSAT project is supported by the German Bundesministerium für Bildung und Wissenschaft (BMBW/DARA) and the Max-Planck-Society. This research has made use of the NASA/IPAC extragalactic database NED) which is operated by the Jet Propulsion Laboratory, Caltech, under contract with the National Aeronautics and Space Administration, and of the SIMBAD database, operated at CDS, Strasbourg, France. The Digitized Sky Survey (DSS) was produced at the Space Telescope Science Institute under U.S. Government grant NAG W-2166.

References

Belloni T., Zampieri L., Campana S., 1997, A&A 319, 525-534
Blaes O., Madau P., 1993, ApJ 403, 690
Bergeron P., Wesemael F., Beauchamp A., Wood M.A., Lamonragne R., Fontaine G., Liebert J., 1994, ApJ 432, 305-325
Colpi M., Campana S., Treves A., 1993, A&A 278, 161
Dame T.M., Ungerechts H., et al., 1987, ApJ 322, 706
Danner R., 1998, A&AS 128, 337
Haberl F., Pietsch W., Motch C., Buckley D.A.H., IAU Circular 6445, 6th August 1996
Helfand D.J., Chanan G.A., Novick R., 1980, Nat 283, 337-343
Madau P., Blaes O., 1994, ApJ 423, 748
Marsh M.C., Barstow M.A., Buckley D.A., Burleigh M.R., Holberg J.B., Koester D., O'Donoghue D., Penny A.J., Sansom A.E., MNRAS 286, 369-383
Motch C., Guillout P., Haberl F., Pakull M., Pietsch W., Reinsch K., 1997a, A&A 318, 111-133
Motch C., Guillout P., Haberl F., Pakull M.W., Pietsch W., Reinsch K., 1997b, A&AS 122, 201-213
Ostriker J.P., Rees M.J., Silk J., 1970, Astrophys. Lett. 6, 179
Stocke J.T., Wang Q.D., Perlman E.S., Donahue M., Schachter J., 1995, AJ 109, 1199
Treves A., Colpi M., 1991, A&A 241, 107
Trümper J., Adv. Space Res. 2, 241
Voges W., Aschenbach, et al., 1996, A&A (in print)
Voges W., 1992, in Proceeding of Satellite Symposium 3, "International Space Year Conference", ESA ISY-3, p. 9
Walter F.M., Wolk S.J., Neuhäuser R., 1996, Nat 379, 233
Zampieri L., Turolla R., Zane S., Treves A., 1995, ApJ 439, 849-853